

Accepted Manuscript

Title: Ni-exchanged Y-zeolite—An efficient heterogeneous catalyst for acetylene hydrocarboxylation

Author: Tie Jun Lin Xuan Meng Li Shi

PII: S0926-860X(14)00466-9

DOI: <http://dx.doi.org/doi:10.1016/j.apcata.2014.07.036>

Reference: APCATA 14929

To appear in: *Applied Catalysis A: General*

Received date: 10-5-2014

Revised date: 14-7-2014

Accepted date: 28-7-2014



Please cite this article as: T.J. Lin, X. Meng, L. Shi, Ni-exchanged Y-zeolite—An efficient heterogeneous catalyst for acetylene hydrocarboxylation, *Applied Catalysis A, General* (2014), <http://dx.doi.org/10.1016/j.apcata.2014.07.036>

This is a PDF file of an unedited manuscript that has been accepted for publication. As a service to our customers we are providing this early version of the manuscript. The manuscript will undergo copyediting, typesetting, and review of the resulting proof before it is published in its final form. Please note that during the production process errors may be discovered which could affect the content, and all legal disclaimers that apply to the journal pertain.

Ni-exchanged Y-zeolite— An efficient heterogeneous catalyst for acetylene hydrocarboxylation

Tie Jun Lin, Xuan Meng, and Li Shi*

The State Key Laboratory of Chemical Engineering, East China University of Science and Technology, Shanghai 200237, People's Republic of China

Highlights

- Production of acrylic acid by the first highly effective heterogeneous catalysts
- The role of metal and acidic sites were investigated
- Promoters such as copper salt can reduce the activation period of the reaction
- The catalytic activity depends on the Ni loading and the state of nickel in zeolite
- Coke formed during the reaction was mainly located outside the channel of zeolite

ABSTRACT:

A series of Ni-modified Y-zeolites with varying Ni loading in the presence of cupric salt as promoter were studied for acetylene hydrocarboxylation performed in a batch reactor. The catalysts were characterized by elemental analysis, H₂-TPR, XRD,

* To whom correspondence should be addressed. E-mail: yyshi@ecust.edu.cn Tel.: 021-64252274.

NH₃-TPD, pyridine-FTIR, SEM, TG-DTG and Raman. It was found that the catalytic activity showed a pronounced dependence on the supports, metal introduction method, promoters and reaction conditions. The nickel species present as charge compensation cations in the zeolite framework constitute the active sites, and the acid sites help to promote the performance of carbonylation. Moreover, two types of coke were observed, and the remarkable reusability of NiY is attributable to the location of the coke outside the zeolite crystals. High catalytic performance was obtained over a NiY(7.0) catalyst with 62 g_{acrylic acid}/(g_{cat}•h) of yield at 235°C, 3.6MPa of initial total pressure and 0.8mM/l of cupric bromide within 40 min of reaction time. This is the most effective heterogeneous system for synthesizing acrylic acid by carbonylation of acetylene to date.

Keywords: Carbonylation, Acrylic acid, Heterogeneous catalysts, Acetylene, Zeolite;

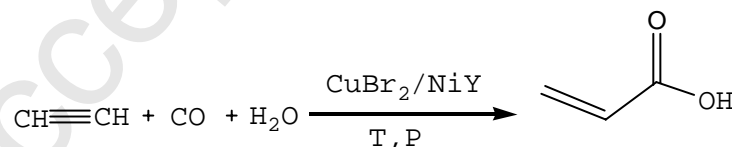
Coke characterization

1. Introduction

In order to reduce the dependence of bulk chemical commodity on natural mineral oil and develop a diversified chemical industry, the coal and alkynes are now again being seen as important alternate raw materials for chemical feedstock.[1,2] Alkynes and, more specifically, acetylene that derived from coal, nature gas or shale gas could be transformed into various base chemicals. [3-5] Among the approaches for these chemicals, one of the most interesting routes is the Reppe carbonylation (Scheme1), known as reaction of acetylene with carbon monoxide and compounds with displaceable hydrogen atoms such as water, alcohols, thiols or amines et al, for

yielding carboxylic monomers [5,7]

Acrylic acid is the primary building blocks of acrylate, polymers, plastics and numerous other industrial and consumer products. The industrial process for producing acrylic acid is based on acetylene carbonylation before the replacement of this route by propylene oxidation.[8] Metal-containing compounds, such as $\text{Ni}(\text{CO})_4$ [7], $\text{NiX}_2\text{-CuX}_2$ ($\text{X}=\text{halogen}$)[9,10], $\text{Ni}(\text{OAc})_2\text{-CuBr}_2\text{-CH}_3\text{SO}_3\text{H-PPH}_3$ [11], are commonly used as active and selective homogeneous catalysts for the acetylene hydrocarboxylation. All of these reported catalysts are dissolved in the solvent media and thus cause the difficulties in the separation of catalyst and product. Recently, as the significant improvement and progress in the design of catalyst and application of new material and reaction technology, the carbonylation of acetylene has been seen as an interesting topic and more recent works were focused on the development of heterogeneous catalysts[12], which would provide the benefit of facile separation of products.[5]



Scheme 1. Hydrocarboxylation of acetylene with CO and water to yield acrylic acid.

The supported nickel catalysts are expected to be effective heterogeneous catalysts for this reaction, and a series of experiments had been done by Bhattacharyya and coworkers[13-16] using nickel salts supported on silica gel as catalyst. It should be noted that, however, the maximum conversion of acetylene by nickel iodide-silica gel catalyst ((Ni/SiO₂= 70/30) is just 8.56%, namely that all of these heterogeneous

catalyst investigated showed little active for the hydrocarboxylation of acetylene to acrylic acid, and much room have been left for us to develop a highly effective solid catalyst systems. It is reported that the both transition metal complex catalyst in homogeneous system and transition metal cations embed in zeolites display catalytic activities in various reactions such as carbonylation[17] and polymerization[18] of acetylene, which suggests some analogies of them in catalytic behavior. Thus, it is supposed that the nickel-modified zeolite would favor the carbonylation of acetylene to acrylic acid.

In this context, it appeared very appealing to investigate the activity of nickel exchanged Y zeolite in the Reppe carbonylation to acrylic acid. In order to understand the role of nickel ions in the catalytic performance, a series of Ni ion-exchanged Y zeolites with varying Ni weight loadings were synthesized and characterized. For comparison, nickel impregnated on SiO₂ and NaY were prepared. Our attention has also focused on the influence of acid sites and reaction conditions on the hydrocarboxylation of acetylene in a batch reactor mode. At last, the solid deposition was also characterized by different techniques.

2. Experimental

2.1 Catalyst preparation.

The starting materials Na–Y zeolite (Si/Al = 3.26, Nankai University catalyst Co., Ltd.), was used as received and in powder form. The nickel-zeolite catalysts were synthesized by two different methods for metal introduction. In the ion-exchange procedure, 10g of NaY was exchanged with 200 mL of 5-200 mM Ni(NO₃)₂ solution.

The exchange was performed at 363 k for 24 h in a round-bottomed flask. After ion exchange, the exchanged zeolite was filtered, washed thoroughly using deionized water, dried at 120°C for 12h, and then calcined in a muffle furnace in static air atmosphere. The resulting zeolite denoted as NiY(x), where x represents nickel mass concentrations. In the incipient wetness impregnation (IWI) procedure, the parent zeolite were outgassed at room temperature under vacuum for 1 h; and then a solution with proper concentration of the Ni(NO₃)₂ was added followed by introducing the impregnated samples into a rotary evaporator under vacuum at 60 °C for 30 min. Subsequently, the dried samples were calcined in air at 550°C for 5 h. The resulting zeolite was denoted as Ni/NaY(x), where x represents nickel mass concentrations. The Ni/SiO₂ with 7.0 wt% of Ni loading was prepared in exactly the same way as the Ni/NaY except the replacement of NaY with silica gel, previously calcined at 550°C. It should be noted that all of the calcined catalysts were not reduced before the activity test.

2.2 Catalyst characterization

2.2.1 Chemical element analysis

The chemical compositions (Ni, Na, Si, Al) in prepared catalyst were determined by inductively coupled plasma atomic emission spectroscopy (ICP-AES, Varian 710ES). The samples were previously dissolved by acid digestion. The content of nickel leached into the liquid was also measured by elemental analysis.

2.2.2 X-ray diffraction

The crystal structure of catalyst was characterized by X-ray diffractometer (XRD,

Bruker D8, Germany) equipped with an atmosphere and temperature control stage and using Cu K α radiation ($\lambda=1.5406 \text{ \AA}$) operated at 40 kV and 100 mA. The scanning range from 10 to 80° (2 θ), 0.02 step, and 1 s/step.

2.2.3 Temperature-programmed Reduction (TPR)

The TPR experiments were performed on a Micromeritics AutoChem II 2920. About 50 mg of catalyst was loaded into a quartz U-tube and dried in Ar atmosphere at 373 K for 1 h before the reduction. The catalyst was then heated in 5% H₂ diluted in argon at flow rate of 30 ml/min with a heating rate of 10 K/min from room-temperature to 1073 K, the consumption of H₂ was monitored using a thermal conductivity detector.

2.2.4 Acidity characterization

The acid properties of samples were measured by ammonia temperature-programmed desorption (NH₃-TPD, Micromeritics 2910) and Fourier transform infrared(FT-IR) spectroscopy (Nicolet company, Model Magna-IR 550). For the NH₃-TPD, The samples was pre-treated in the stream of helium (50ml/min) at 450 for 2h and afterwards cooled to 180 °C and then saturated under an ammonia stream for 30 min. The physically adsorbed ammonia was removed by flowing He with 50ml/min at 180°C for 90min. Subsequently, the sample was heated to 550°C at 10°C/min in flowing He to remove the chemically adsorbed ammonia. The amount of desorbed ammonia was continuously monitored with a thermal conductivity detector (TCD). For the pyridine-FTIR, the characteristic absorption peak of Brønsted acid is located at 1540 cm⁻¹, and that of Lewis acid is located at 1450 cm⁻¹. The detailed information

about the identification and determination of acid amount, acid density and acid variety can be found elsewhere. [19]

2.2.5 Thermal analysis

The fresh and recovered catalysts were measured by thermo-gravimetric analysis (TGA). The sample were loaded on a platinum microcrucible and were heated up to 800 °C at 10 °C/min with flowing air at 100 ml/min, recording continuously the weight of each sample.

2.2.6 SEM and Raman spectra

The morphologies of recovered catalysts were obtained using a Nova Nano SEM450. A Micro-Raman System (HORIBA Jobin Yvon) using He-Ne laser beam with a wavelength of 632nm was used to analyzing the nature of coke in the spent catalyst. The quality was identified by Raman spectroscopy using the 514nm line of an argon laser operated at a laser power of 50 MW.

2.3 Hydrocarboxylation procedure

The catalytic hydrocarboxylation of acetylene was performed in a 0.5L Parr autoclave made of stainless steel-316 having facilities for gas inlet and outlet, a rupture disk as a safety measure in case of excessive pressure buildup, intermediate sampling, temperature-controlled heating, and variable agitation speed.

In a typical experiment, known quantities of catalyst powders (0.5g), promoters (0.08mM/l), H₂O(15ml) , and acetone (150ml) were charged into a stirred pressure reactor. The reactor was firstly flushed with nitrogen for several times and subsequently pressurized with acetylene to 0.5MPa and then to 3.6 MPa of initial total

pressure with CO (both controlled by mass flowmeter) at room temperature. The reactor was then heated to 235°C and the reaction proceeded until no pressure drop was observed under constant agitation (800 rpm). After the reaction, the autoclave was quickly cooled to room temperature and the tail gas and liquid were collected, calculated and analyzed. For recycling experiments, the catalyst used in the previous run was separated by filtration and washed with acetone for several times and reused after drying under vacuum. The detailed schematic drawing of the reactor is shown in Fig. S1 (supplemental materials).

The conversion of acetylene, selectivity and yield of acrylic acid and the space time yield (STY) are defined as follows:

$$\text{Conversion} = \frac{n_0 - n_1}{n_0} \times 100\%, \quad \text{Selectivity} = \frac{n_p}{n_0 - n_1} \times 100\%, \quad \text{Yield} = \frac{n_p}{n_0} \times 100\%$$

$$\text{STY} = \frac{g_{AA}}{g_{cat.} \cdot h} \times 100\% \quad \text{or} \quad \text{STY} = \frac{g_{AA}}{\text{molNi} \cdot h} \times 100\%$$

Where, n_0 , amount of acetylene for feedstock before reaction; n_1 , amount of acetylene for residue after reaction; n_p , amount of acetylene for forming acrylic acid; g_{AA} , the amount of acrylic acid produced during reaction; $g_{cat.}$, the amount of catalysts for input before reaction; molNi , the molar content of nickel contained in the catalysts for input before reaction.

3. Results and discussion

3.1 Characterization of Catalyst

The chemical elements of Na-Y and Ni-exchanged Y zeolite were determined by element analysis. The Ni loading, degree of site exchange, and the ratio of total

silicon to aluminum are present in Table 1. Fig. S2(supplemental materials) shows the effect of $\text{Ni}(\text{NO}_3)_2$ concentration in the exchange aqueous solution on the Ni loading in NiY. As can be seen, the Ni loading nearly increases linearly with an increase in $\text{Ni}(\text{NO}_3)_2$ concentration from 5mM to 60mM, and almost remains unchanged with a further increase in the $\text{Ni}(\text{NO}_3)_2$ concentration, which suggests that the Ni loading can be controlled by varying the $\text{Ni}(\text{NO}_3)_2$ concentration in the aqueous solution. The maximum exchange degree was determined to approximately 62% and the corresponding Ni loading was 7.0 wt% in this study. It is reported that the metal cations introduced to the zeolite by ion-exchange process are in the form of a skeleton balance-charge, namely that one Ni^{2+} cation exchanged into the zeolite charges compensate two change sites, and thus ratio of $n(2\text{Ni}^{2+} + \text{Na}^+)/n(\text{Al})$ should be a constant value (≈ 1.0)[19], which is consistent with the results showed in Table 1. Moreover, the observation that the increase in $n(\text{Si})/n(\text{Al})$ ratio from 3.26 to 3.28 indicates the ion-exchange process caused slightly collapse of the molecular sieve structure and dealumination of the framework.

X-ray diffraction technology was used to characterize the physicochemical properties of the NaY, Ni/NaY and Ni-exchanged Y zeolite with various Ni loadings, the result is shown in Fig. 1. There is no significant structural modification after nickel ion exchange compared to the parent NaY. However, the X-ray diffraction peaks of the NiY samples are less intense, indicating the slightly decrease in the crystallinities of zeolite during the exchange process and subsequent calcination. The XRD patterns only show characteristic diffraction peaks of NaY, and none of nickel

oxide or other nickel species is detected. All of these facts suggest that the nickel ions exchanged into the zeolite samples resided as charge-compensating and the nickel ions were highly dispersed in exchanged zeolite. While for the Ni/NaY prepared by incipient wetness impregnation (IWI), the characteristic peaks of NiO at 2θ of 37.25° , 43.28° and 31.44° (JCPDS47-1049) were clearly observed, indicating that the nickel ions mainly present as in the form of bulk NiO on the impregnated catalysts.

The TPR spectrum of Ni/NaY prepared by IWI and Ni-exchanged Y zeolite are shown in Fig.2. For NiY catalyst after calcination, the spectrum exhibits only one high temperature strong reduction at approximately 1043K, which is attributable to the reduction of charge-compensating Ni^{2+} cations. The similar result was observed for Ni-exchanged other zeolites.[21,22] While for the Ni/NaY sample, one weak reduction peak at high temperature zone (756 K) and three reduction peaks composing of one strong reduction peak at about 450K and two weak shoulder weak at appropriately 823K and 1043K, respectively, are observed. According to the literatures[23], the former peak is attributable to the reduction of bulk NiO particles located mainly outside the pores of zeolite support[22], the latter two reduction peaks may correspond to the presence of smaller NiO particles located inside the channels of zeolite, which are less reducible caused by a stronger metal-support interaction than the bulk NiO particles.[24] The reduction peak at 756 K is analogous to that observed in ion-exchanged NiY samples and is attributed to the reduction of nickel located inside the framework of zeolites. These facts clearly indicates that all of the Ni cations in NiY are distributed exclusively as charge-compensation cations in the

zeolite framework, as shown in Fig. 4, while most of Ni ions are dispersed on the outer surface and presented as the form of NiO in the impregnated catalyst after calcination, and fewer nickel ions were introduced into the zeolite framework as compensation cations during the IWI process[25]. These nickel species distributed as compensation cations are difficult to reduce and require higher reduce temperature than that of nickel oxide particles.[26]

Ammonia TPD profiles of parent NaY, NiY, Ni-NH₄Y and Ni-HY are plotted in Fig.4. Fig. S3 (Supplementary Material) shows the Pyridine-FTIR spectra of the NaY and NiY at 200°C and 450°C, and the quantification results of their acid properties characterized by Pyridine-FTIR are listed in Table 2. It is evident that the acidic properties of zeolite changed during the ion exchange of Na⁺ with Ni²⁺. For the parent NaY, only one large ammonia desorption band between 50~200°C with a maximum intensity at about 125°C is observed, which is assigned to the weak acid sites and further confirmed to be weak Lewis sites by pyridine-FTIR. The ammonia desorption at about 300 and 425°C, respectively, indicates the occurrence of medium and strong acid sites in sample after Na ions are substituted by nickel ions. From the results of pyridine-FTIR, the total number of acid sites and, specifically, Lewis acid increases significantly, which is agreement with the point proposed by Minchev et al[27] that the nickel cations play the role of Lewis acid centers. Moreover, the additional Brønsted acid sites would be formed and each Ni²⁺ produces two acid sites after Ni²⁺ ion exchange of Na-zeolite. [28-30] The acidity of Ni-NH₄Y and Ni-HY is measured by NH₃-TPD to explain the role of acid sites on the hydrocarboxylation of acetylene,

and this aspect will be discussed in the next section.

3.2 Catalytic activity

3.2.1 Role of nickel sites

It had been disclosed that^[9]the production of acrylic acid by bring acetylene and carbon monoxide into contact with water in the presence of compounds of metals of VIII Group, i.e. iron, nickel and cobalt can be carried out at elevated pressures and temperatures. To stand out the role of metals in the acetylene hydrocarboxylation, various catalysts including FeY, CoY, NaY, HY, Ni/SiO₂, Ni/NaY(imp.,3.1), Ni/NaY(imp.,7.0) , NiY(7.0) ,Ni-NH₄Y and Ni-HY were tested. As can be seen from the Table 3, all of Ni free samples were completely inactive for acetylene hydrocarboxylation within 2 hours, whereas the Ni-containing catalysts showed varied degree of activity under the identical conditions, suggesting that the nickel sites play an indispensable role in the activity of acetylene hydrocarboxylation. As concern the nickel-base catalysts, it was found that the supports and metal introduction methodology have a great influence on activity. The reaction rate of NiY(ion-exchange, 7.0) was four times of that of Ni/NaY(imp.7.0). These differences may be attributable to the different state of nickel species in the catalysts. For the catalysts prepared by impregnation, the bulk NiO species existed on the zeolite are considered to be low activity for the carbonylation of acetylene. Interestingly, Huang et al^[31-33] hold that the NiO are the active species in hydroesterification of acetylene with CO and methyl formate to yield methyl acrylate. Further comparison between the Ni/NaY and Ni/SiO₂ (both prepared by incipient wetness impregnation), the higher

activity of the former is because of some nickel ions distributed as charge-compensate in the framework of zeolite (verified by TRR result in Fig. 2) during the preparation process using NaY as support, and those parts of Ni^{2+} work more in the reaction, while only NiO species were detected in Ni/SiO₂ sample. What is noteworthy is that the Ni/NaY with 7.0 wt% Ni loading shows lower activity than that with 3.0 wt% Ni loading after calcination, which indicates that the formation of nickel oxide become favored when raising the nickel amount via impregnation, the similar phenomena were observed and confirmed by Maia et al.[23]

The high activity of NiY prepared by ion-exchange among the investigated catalysts further demonstrates the dominant role of Ni species distributed as compensation cations in the reaction. In order to further investigate the effect of Ni loading on the activity, the NiY with different degrees of exchange were compared.

The tested reaction is terminated when no pressure drop was observed, and the reaction time for each run was 120 min, 90 min, 64 min, 44 min and 40 min, respectively. As shown in Fig. 4, the yield and space time yield (STY) increase with the increase in Ni loading. For the NiY with Ni loading exceeds 3.1wt% (corresponding to 28% of exchange degree), no obvious changes were observed in yield, but significant increase in the STY, indicating that the samples with lower Ni loading require more time to acquire the same targeted product yield. On one hand, there are no enough active molecules that can coordinate with reactants for these catalysts with lower nickel loadings; on the other hand, the possible migration of nickel ions from inaccessible hexagonal prism and sodalite cages to zeolite supercage

within the zeolite during the reaction would also account for this. In regard to these NiY catalysts with the degree of cation exchange less than 40% (NiY(0.8), NiY(3.1)), the Ni cation resides mainly inside the hexagonal prisms and sodalite cages, or SI and SII sites of the faujasite zeolite, respectively, these Ni²⁺ cations are not active for the reaction due to their inaccessibility to the reactant.[22,34] Under the reaction conditions, the Ni cations will migrate into the supercage from SI sites and work with reactants to form active sites. For these samples with higher exchange degree, the Ni cations would locate directly in the zeolite supercage, and thus require less time to activate the reaction. The pressure-time plot (Fig S4, supporting materials) for these catalysts with different nickel loadings agreed well with our hypothesis.

3.2.2 Effect of reaction temperature and initial total pressure

Fig.5(a) presents the effect of reaction temperature on the hydrocarboxylation of acetylene using NiY(7.0) as catalyst. The run was carried out in acetone, at 3.6MPa of initial total pressure with reaction temperature selected at 200°C, 220°C, 235°C and 250°C, respectively. No acrylic acid was detected at a temperature of about 200°C after 2h of reaction time. As the temperature increased to 220°C, the yield of acrylic acid enhanced drastically and the yield goes through a maximum at about 235°C (40 min of reaction time). With further increase of temperature to 250°C, however, the pronounced fall in space time yield (STY) was observed. After separation by filtration, obvious coke deposition and polymer were observed, which suggests that the occurrence of polymerization and decomposition of acetylene and/or acrylic acid. We note that the similar phenomena were observed by Bhattacharyya,[14] and these

sediments would cause serious problems, thus a proper temperature of about 235°C was selected in this reaction.

The effect of initial total pressure on the activity in the acetylene hydrocarboxylation was investigated under the same molar ratio of CO/C₂H₂, and the result is shown in Fig. 5(b). As expected, the activity increased drastically by increasing the initial total pressure from 2.5 to 3.6 MPa. The higher pressure will increase the solubility of gas in the liquid, and favor its contact and coordination with metal ions in the zeolite catalyst and to form active species. But on further increase in the initial pressure will cause the decomposition of acetylene and bring the operational risk and cost, so the further experiments will be performed at 3.6 MPa of initial total pressure.

3.2.3 Role of copper salt

The catalytic properties of NiY(7.0) with a variety of copper salt as promoter were evaluated for the hydrocarboxylation of acetylene under the same conditions at 235 °C, 3.6MPa of initial total pressure and acetone as solvent. As can be seen from the Fig. 6(a), different copper salts displayed varied catalytic activity. Among these promoters investigated, the cupric bromide gave the best activity, while the substitution of bromide with acetate or nitrate proved counterproductive and led to decreased production of acrylic acid and increased production of unwanted polymer. Cupric halide(CuX₂) and cuprous halides(CuX) were all found to be effective in improving the carbonylation, but gave the different activities depend on the halogen ions. It has been reported that the cupric ion plays an important role in activating the

acetylene[11,20]. Thus, the differences between these tested copper salts could be attributed to their different coordinative behaviors with acetylene. Some copper salts tend to cause the formation of polymer and that would be trapped near the entrance of the channels or cages and therefore result in the problems of mass transfer. Fig. 6(a) also indicates that bromide ion plays a special role in the forming intermediates. Exact nature of the influence of bromide ion is unknown. It may be speculated that the bromide ion serves as a bridge between cupric ion and acetylene and thus increasing the kinetics of electron transfer and stabilizing the copper-acetylide species and favoring its attack and insertion to $\text{Ni}^{2+}-(\text{CO})_n$ intermediates species. Moreover, the cupric bromide is deemed to improve the solubility of carbon monoxide[11] and thus increasing the diffusion rate of gas into to liquid-phase. Note that the improvement of reaction rate by introducing the copper salts into the catalyst system was also observed in other types of reaction.[35,36]

In order to further explain the role of cupric bromide, the effect of its concentration was studied and the result was shown in Fig. 6(b). As can be seen, a marked increase in the conversion of acetylene is observed with increase in cupric bromide concentration from 0 to 0.8 mmol/l(mM/l), and the conversion increases slightly with further increase in the concentration. The increase of selectivity to acrylic acid from 58% to 81% with the increase of concentration of CuBr_2 indicates that the copper plays a positive role in the carbonylation of acetylene. However, the selectivity decreases drastically when the concentration of CuBr_2 exceeds 0.8mM/l. In consideration of the change trend of conversion and additional byproducts detected in

gas chromatography and precipitate in the products, it can be inferred that the excess of cupric salt resulted in the decomposition of acetylene and the formation of polymer. That is, the cupric salt plays a double role in the carbonylation process, and the suitable concentration should be controlled.

3.2.4 Influence of acid sites

It is of importance to clarify the role of acid sites in the hydrocarboxylation of acetylene. Most of the previous studies of acetylene reaction are carried out on acidic zeolites[37,38], and it is believed that the acetylene is easy to interact with acid sites forming hydrogen-bound species[39]. Thus, it is necessary to answer the question about whether the presence of acid sites is required in this reaction. For this purpose, a special experiment run was carried out in the presence of Ni-NH₄-Y catalyst, which is the non-calcined Ni-HY sample. The NH₃-TPD profiles of Ni-NH₄Y and Ni-HY are shown in the Fig. 3. Compared to NH₄-form catalyst, the H-form sample shows a higher density of weak, medium and strong acid sites. Table 3(entry 8 and entry 9) gives the comparative results of catalytic performance of Ni-NH₄Y and Ni-HY. It is evident that the Ni-NH₄Y shows relative lower catalytic activity, while the Ni-HY gives a better result. It is noteworthy that the coke deposition in the recovered Ni-HY is a little more, indicating that the higher density of acid sites are more likely to cause the decomposition of acetylene. In addition, a Ni-SiO₂ (the Ni is present solely as isolated Ni²⁺ after impregnation and calcination rather than bulk NiO in the catalyst) without acid sites were prepared according to the literature[22], and it is found that the catalytic activity towards acrylic acid is very low. These findings suggest that the

acid sites have a certain effect on the catalytic performances, and the moderate density of acid sites helps to promote the carbonylation. A possible explanation is that the acid sites would interact with acetylene and promote the protonation of acetylene to form active intermediates.

3.2.5 Stability of catalyst

Reusability is crucial for prospective uses in a continuous tubular reactor and further applications in industrial scale. No information is available regarding the stability and recyclability of zeolite catalysts in liquid-phase hydrocarboxylation of acetylene and herein we firstly report the results for the most promising NiY(7.0) catalyst.

Table 4 gives the reusability test of NiY catalyst for several repeated run. It is surprising that the catalytic activity remained stable over four consecutive runs. No obvious loss in the conversion and selectivity towards acrylic acid was observed, notwithstanding the catalyst powder, which was originally white, turned black because of coke formation and accumulation after the fourth catalytic run. Interestingly, upon removal of the deposits through calcination at 823 K for 5h, the catalytic performance of heat-treated NiY(7.0) catalysts was identical to that of pristine catalysts, suggesting that a great part of the coke is located on the external surface of the zeolite catalyst. Moreover, a very small amount of Ni ions (less than 0.3ppm) in the reaction liquid detected by ICP-AES indicates the stability of nickel ions exchanged into the framework of zeolite.(seeing Fig S5 in the supplementary materials)

In order to study the state of catalysts after reaction, the recovered catalysts were characterized by XRD and TPR. Fig. 7 gives the X-ray diffraction patterns of the fresh and recovered NiY catalyst. No obvious peaks changing in XRD and TPR (not shown here) profile were observed between them, indicating that the state of nickel remains nearly unchanged during the reaction. Although the types of peak in XRD patterns remain unchanged, the slightly decrease in intensity of peak for the recovered catalyst may be caused by the slightly decrease in the crystallinities of zeolite and collapse in zeolite structure during the reaction or by the coke or some polymer deposited on external surface of zeolites.

3.3 Characterization of solid deposition

Coke deposition and polymer are the most common and serious problem in the hydrocarboxylation of acetylene under elevated temperature and pressure. In the preceding study[20,40], the formation of solid deposition in the homogeneous system was detailed studied, and the amount of sediments strongly depend on the catalysts used and reaction conditions. The deposition, mainly referred to coke, in zeolites is formed mainly due to the decomposition and/or polymerization of acetylene. The coke may be located both on the external surface and inside the channels of the zeolites. In this section, the fresh and recovered catalysts were characterized by a number of techniques, such as TG-DTG, SEM and Raman, in order to gain information about the nature of the coke.

The TG and DTG results from the temperature-programmed oxidation of the tested samples are shown in Fig.8. As can be seen from Fig.8(B), a large peak ranges of

50~200°C in all of the tested samples is attribute to the moisture vaporization peak, and none of other peaks can be found in the fresh NiY and parent NaY sample. The amount of coke can be roughly calculated according to the weight loss of sample between 200°C to 700°C. It is apparent that the amount of coke in the recovered Ni/NaY is larger than that of NiY sample calculated based on the TG analysis shown in Fig.8(A). In the case of NiY, the amount of coke is about 12% referred to the used zeolite sample, which is higher than the maximum amount of that could be accumulated inside the NiY zeolite micropores. Considering the observation of a small amount of black particles in the recovered catalyst and remarkable reusability of the catalyst, it can be inferred to that most of this coke is deposited over the external surface of zeolite, and the active site remain accessible for the reactant molecules. Moreover, based on the previous study[20], the decomposition of acetylene is mainly caused by the copper salt. For those activated acetylene outside the zeolite channel, it is easy to decompose, but if they transfer to the zeolite micropores and function with the metal site, the acetylene becomes more stable. Namely, the reaction towards the carbonylation is superior to decomposition for the acetylene coordinated with the Ni site inside the zeolite supercage.

The profile of derivative of the TG weight loss as a function of temperature shown in Fig.8(B) also provides information about the location and nature of the coke deposits. From the DTG profile, two exothermic peaks were observed at the temperature ranges from 200 to 500°C for the catalyst prepared by incipient wetness impregnation and ion-exchange. No obvious oxidation peak was found at temperature

exceeds 550°C. All of these facts suggest that there are two types of deposition exist in the spent catalyst. The first type of coke, soft coke or polymeric coke, can be removed at a relative lower temperature, while the remove of the second coke (refractory coke) need higher temperature. [41-42] In terms of the location of coke, the oxide peak at around 300°C may correspond to the burn out of coke deposited on the external surface of the zeolite, and the relatively broader peak indicates that there is little coke deposited within the zeolite micropores.

SEM results of fresh and recovered catalyst are shown in Fig. 9. It is evident that the zeolite retains its microstructure as octahedral or hexagonal prism sheet structure before and after reaction, but the location, morphology and nature of coke show some differences. In the case of the recovered NiY samples, the coke deposited on the surface of the zeolite is assigned to filamentous coke, which is in the form of carbon nanotubes with filamentous lines structures. Most of those nanotubes are separated from the zeolite crystals and tend to aggregate to form clusters (Fig. 9(b)). The feature of the coke location in the zeolite explains why the NiY catalysts keep a remarkable catalytic activity after several times of consecutive catalytic run. But for the recovered Ni/NaY(imp.) samples(Fig. 9(c,d)), most of the zeolite grain are covered by a layer of tiny particles. Moreover, the filamentous coke is also found in this sample. These facts imply that the different formation mechanism of coke between NiY and Ni/NaY(imp.) catalyst. The results of SEM analysis of these samples are line with the findings in the TG-DTG analysis, and are agreement with the above results of reusability test of catalyst.

Additional information about the nature of coke in the recovered NiY catalyst can be obtained from the Raman characterization. As shown in the Fig. 10, there are two large bands can be observed at 1360 and 1596 cm^{-1} in the spectra of the recovered catalysts, which are known as D-band and G-band, respectively. The feature of the coke characterized by Raman is the same as that observed in the homogeneous system. [20]The G-band provides information about the electronic properties of the filamentous carbon and is used to characterize the ordered carbon, while the D-band is usually used to characterize the polycrystalline and imperfect graphite and other types of carbon. The Raman spectra also indicates that the nanotubes observed by SEM present multiwalled morphology.[43] In a word, the Raman profiles clearly indicates that the coke formed on the NiY present as quite different nature, as above concluded from TG-DTG results.

4. Conclusion

The Ni-modified Y-style zeolites were examined as a case of highly efficient heterogeneous catalyst for the hydrocarboxylation of acetylene with carbon monoxide and water to yield acrylic acid.

A careful comparison of catalysts prepared by different supports and nickel introduction methodologies (incipient wetness impregnation and aqueous ion exchange) reveals that the Ni-exchanged Y zeolites with the presence of cupric salt as promoter give the best catalytic activity ($62 \text{g}_{\text{acrylic acid}}/(\text{g}_{\text{cat}} \cdot \text{h})$). The multiple reuse of NiY with stable activity in a batch reactor was demonstrated at 235°C and 3.6MPa of initial total pressure in a short period of reaction time.

The catalytic activity shows a pronounced dependence of the reaction conditions. The reaction velocity increases with the initial total pressure increases from 2.5 to 3.6 MPa. The temperature exceeds 250°C would cause the obvious decomposition of acetylene and thus the decrease in the selectivity to acrylic acid, and that under 220°C would bring about the lower reaction rate. The types of copper salt influence the yield of target production, and the activity goes through a maximum using cupric bromide as promoter.

Elemental analysis, XRD and TPR characterization indicates the nickel introduced into the zeolite framework presents as charge-compensation, and remains the state throughout the reaction. The loading of Ni in the zeolite can be controlled by controlling the concentration of nickel nitrate in the aqueous exchange solution. It is found that the bulk NiO is detrimental to the reaction, while the Ni²⁺ ions in a high coordinative unsaturation in the zeolite are proposed to be catalytic sites in acetylene hydrocarboxylation. Pyridine-FTIR and NH₃-TPD suggest that the acidity of NiY increases remarkable after ion-exchange compared with parent NaY, and the moderate acidity favors the protonation of acetylene.

Characterization of recovered catalysts by TG-DTG, SEM and Raman indicate that the different coke amount and location between NiY and Ni/NaY(imp.) catalysts. The coke deposition on NiY presents a relative ordered filamentous nature, and much of them located mainly outside the zeolite crystals and thus keeps a remarkable reusability in spite of the relative higher amount of coke deposited after many times of recovery.

Acknowledgement

We are grateful for the financial support from China Postdoctoral Science Foundation (No: 2013M541488) and Opening Project of State Key Laboratory of Chemical Engineering of East China University of Science and Technology (No. SKL-ChE-11C04).

Appendix A. Supplementary data

Supplementary data associated with this article can be found in the online version.

References

- [1] A.Corma, Chem. Rev. 114(2014) 1545–1546.
- [2] Nexant Incorporation, Multiclient Prospectus-Chemicals from acetylene, back to the future? <http://www.nexant.com/>, 2007.
- [3] R.Chinchilla, C.Nájera, Chem. Rev. 114(2014) 1783–1826.
- [4] H. Schobert, Chem.Rev. 114(2014) 1743–1760
- [5] I.T. Trotaş, T. Zimmermann, F. Schüth, Chem. Rev. 114(2014) 1761– 1782.
- [6] G. Kiss, Chem. Rev. 101(2001) 3435– 3456.
- [7] W. Reppe, Acetylene Chemistry, Meyer, New York, 1949.
- [8] R.J. Tedeschi, Acetylene-Based Chemicals from Coal and Other Natural Resources, Marcel Dekker, New York, 1982.
- [9] W. Repee, R. Stadler, US Patent 3023237(1962).
- [10] K. Weissmehl, H.J. Arpe, Industrial Organic Chemistry, Wiley-VCH, Weinheim, Germany,1993, pp. 272.
- [11] C.M. Tang, Y. Zeng, P. Cao, X.G. Yang, G.Y. Wang, Catal.Lett. 129(2009)

189-193.

- [12] C.M. Tang, P. Cao, Y.Zeng, X.G. Yang, G.Y. Wang, *Petrochemical Technology*, 37(2008) 1089-1094.
- [13] S.K. Bhattacharyya, A.K. Sen, *Journal of Chemical Technology and Biotechnology* 13(1963) 498–505.
- [14] S.K. Bhattacharyya, A.K. Sen, *Ind. Eng. Chem. Proc. Des. Dev* 3(1964) 169–176.
- [15] S.K. Bhattacharyya, D.P. Bhattacharyya, *J. Appl. Chem.* 16(1966) 18–21.
- [16] S.K. Bhattacharyya, D.P. Bhattacharyya, *J. Appl. Chem.* 16(1966) 202–205.
- [17] S.L. Phillip, N.J. Woodbury, US Patent 3334132 (1967).
- [18] P. Pierre, C.V. Jacques, G. Pierre, I. Boris, *J. Catal.* 32(1974) 190–203.
- [19] D.Z. Yi, H. Huang, X. Meng, L. Shi, *Appl. Catal. B: Environm.* 148-149(2014) 377–386.
- [20] T.J. Lin, X. Meng, L. Shi, *Ind. Eng. Chem. Res.* 52(2013) 14125–14132.
- [21] V. Hulea, F. Fajula, *J. Catal.* 225(2004) 213–222.
- [22] A.N. Mlinar, G.B. Baur, G.G. Bong, A. Getsoian, A.T. Bell, *J. Catal.* 296(2012) 156–164.
- [23] A.J. Maia, B. Louis, Y.L. Lam, M.M. Pereira, *J. Catal.* 269(2010) 103–109.
- [24] C. Wu, L. Wang, P.T. Williamsa, J. Shi, J. Huang, *Appl. Catal. B: Environm.* 108–109(2011) 6–13.
- [25] A. Carrero, J.A. Calles, A.J. Vizcaíno, *Appl. Catal. A: Gen.* 327(2007) 82–94.
- [26] B. Pawelec, R. Mariscal, R.M. Navarro, J.M. Campos-Martin, J.L.G. Fierro,

- Appl. Catal. A: Gen. 262(2004) 155–166.
- [27] C. Minchev, S.A. Zubkov, V. Valtchev, V. Minkov, N. Micheva, V. Kanazirev,
Appl. Catal. A: Gen. 119(1994) 195–204.
- [28] B.I. Mosqueda-Jiménez, A. Jentys, K. Seshan, J.A. Lercher, Appl. Catal. B:
Environm. 46(2003) 189–202.
- [29] B.I. Mosqueda-Jiménez, A. Jentys, K. Seshan, J.A. Lercher, J. Catal. 218(2003)
375–386.
- [30] M.O. Lallemand, A. Rusu, E. Dumitriu, A. Finiels, F. Fajula, V. Hulea, Appl.
Catal. A: Gen. 338(2008) 37–43.
- [31] X.H. Huang, X.G. Yang, J.Q. Zhang, Z.T. Liu, Chinese Chem. Lett. 11(2000)
521–524.
- [32] X.H. Huang, X.G. Yang, J.Q. Zhang, Z.T. Liu, J. Nat. Gas. Chem. 10(2001)
42–50.
- [33] X.H. Huang, Z.T. Liu, J.Q. Zhang, X.G. Yang, J.W. Wang, J. Nat. Gas. Chem.
9(2000) 197–204.
- [34] P. Gallezot, B. Imelik, J. Phys. Chem. 77(1973) 652–656.
- [35] B.C. Dunn, C. Guenneau, S.A. Hilton, J. Pahnke, E.M. Eyring, Energy & Fuels
16(2002) 177–181.
- [36] J.L. Hu, Y.L. Gu, Z.H. Guan, J.J. Li, W.L. Mo,; T. Li, G.X. Li, ChemSusChem
4(2011) 1767–1772.
- [37] C. Pereira, G.T. Kokotailo, R. J. Gorte, J. Phys. Chem. 95(1991) 705–709.
- [38] P. Tsai, J.R. Anderson, J. Catal. 80(1983) 207–214.

- [39] G. Onyestyák, L.V.C. Rees, *Appl. Catal. A: Gen.* 223(2002) 57–64.
- [40] J.M. Qiu, Y.Z. An, D.H. Yang, L.R. Feng, *Nat. Gas Chem. Ind.* 19(1994) 10–14.
- [41] J.J. Guo, H. Lou, X.M. Zheng, *Carbon* 45(2007) 1314–1321.
- [42] X.J. Zhang, Y. Wang, F. Xin, *Appl. Catal. A: Gen.* 307 (2006) 222–230.
- [43] A.M. Rao, E. Richter, Shunji Bandow, Bruce Chase, P.C. Eklund, K.A. Williams, S. Fang, K.R. Subbaswamy, M. Menon, A. Thess, R.E. Smalley, G. Dresselhaus, M. S. Dresselhaus, *Science* 275(1997) 187–191.

Table 1 Elemental analysis of Na-Y and Ni-Na-Y exchanged with different Ni(NO₃)₂ concentration

Sample	Elemental analysis		Si/Al	Cations/Al ^a	% Exchange ^b
	(wt%)				
	Ni	Na			
NaY	0.0	8.97	3.26	0.99	0
NiY (5mM) ^c	0.8	8.3	3.26	0.99	7
NiY (20mM)	3.1	6.44	3.27	0.98	28
NiY (60mM)	6.8	3.60	3.28	0.99	60
NiY (200mM)	7.0	3.45	3.28	0.99	62

^a Calculated assuming that every positive charge from the exchanged cations can charge compensate an exchange site ((Na+2Ni²⁺)/Al);

^b Determined as the amount of Na⁺ replaced by the exchanged cation Ni.

^c NiY(x), x represents the concentration of Ni(NO₃)₂ in the exchange aqueous solution

Table 2 Acidic properties of NaY and NiY (7.0) calculated according to the result of Pyridine-FTIR spectra $\times 10^{-4}$ mol g $^{-1}$).

Sample	T	T _L	T _B	S _B	S _L	W _B	W _L
Na-Y	1.95	1.95	0	0	0	0	1.95
Ni-Y (7.0)	20.5	17.46	3.04	0	1.44	3.04	16.02

T—Total acid; T_L—total Lewis acid; T_B—total Brønsted acid; S_L—strong Lewis acid; S_B—strong Brønsted acid; W_L—weak Lewis acid; W_B—weak Brønsted acid.

Table 3 Comparison of the catalytic performance of various catalysts

Entry	Catalyst	Reaction time	Activity
		/min	($\times 10^4$) $g_{AA}/(\text{molNi} \cdot \text{h})$
1	FeY	120	0.00
2	CoY	120	0.00
3	NaY	120	0.00
4	HY	120	0.00
5	Ni/SiO ₂	120	0.10
6	Ni/NaY(7.0)	120	1.16
7	Ni/NaY(3.1)	90	1.36
8	Ni-NH ₄ -Y	50	3.45
9	Ni-H-Y	40	4.06
10	Ni-Na-Y(7.0)	40	5.05

Table 4 Reusability test of NiY(7.0) catalyst

Catalyst	Promoter	Times of usage	STY
			($\times 10^4$) $G_{AA}/(\text{molNi} \cdot \text{h})$
NiY	CuBr ₂	1	5.13
		2	5.06
		3	5.20
		4	5.13
		5 [*]	5.12

5^{*}:The catalyst was recovered after the fourth catalytic run and then calcined at 823k for 5h in air and subsequently put into the reactor for the next reaction.

Fig. captions:

Fig. 1. X-ray diffraction patterns of parent NaY and calcinated NiY catalyst with different Ni loading

Fig. 2. TPR profiles of NiY and Ni/NaY catalysts. The peak at about 450 °C is due to the reduction of bulk NiO, the peak at 500~650 °C is attributed to the reduction of Ni ions located inside the channels of zeolite, the peak at 756 °C and 770 °C is due to the reduction of Ni sites incorporated into the zeolite framework

Fig. 3. NH₃-TPD profiles of NaY, NiY, Ni-NH₄Y and Ni-HY

Fig. 4. Effect of Ni loading on catalytic activity (Reaction time: 120min for NiY(0), 90min for NiY(0.8), 52min for NiY(3.1), 44min for NiY(6.8), 40 min for NiY(7))

Fig. 5. Effect of reaction temperature (a) and initial total pressure (b) on the catalytic activity

Fig. 6. Role of promoters in the hydrocarboxylation of acetylene: Effect of copper salts (a) and concentration of CuBr₂ (b) on the catalytic activity

Fig. 7. X-ray diffraction patterns of the fresh and recovered NiY catalyst

Fig. 8. Thermo gravimetric analysis of the fresh and spent Ni modified zeolite catalysts by ion-exchanged and wet impregnation: (A) weight loss as function of temperature (TG) and (B) derivative weight loss as function of temperature (DTG)

Fig. 9. SEM micrographs of fresh NiY(a) , recovered NiY(b) and recovered Ni/NaY(c,d)

Fig. 10. Raman spectra of the recovered NiY catalyst

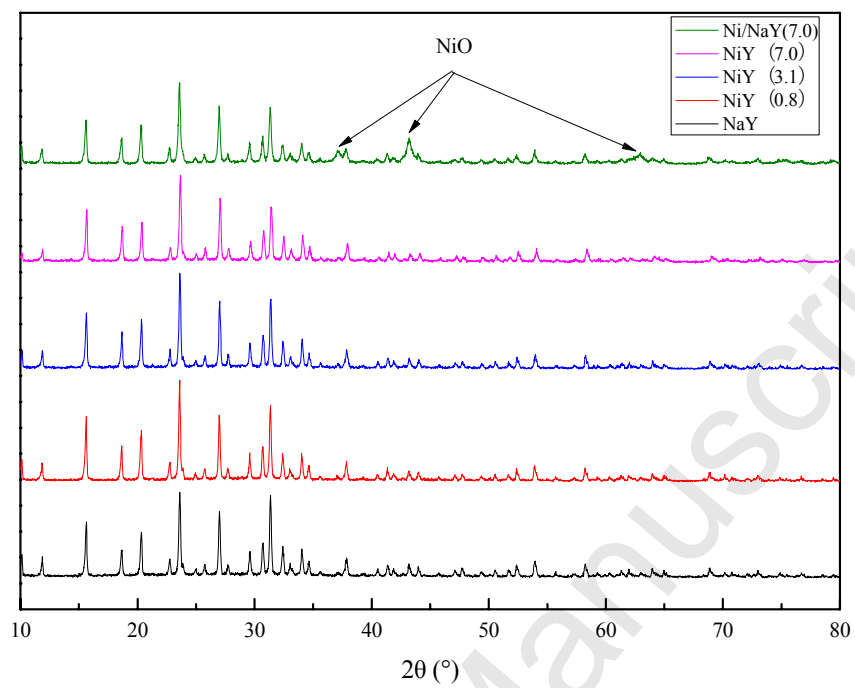


Fig. 1. X-ray diffraction patterns of parent NaY and calcinated NiY catalyst with different Ni loading

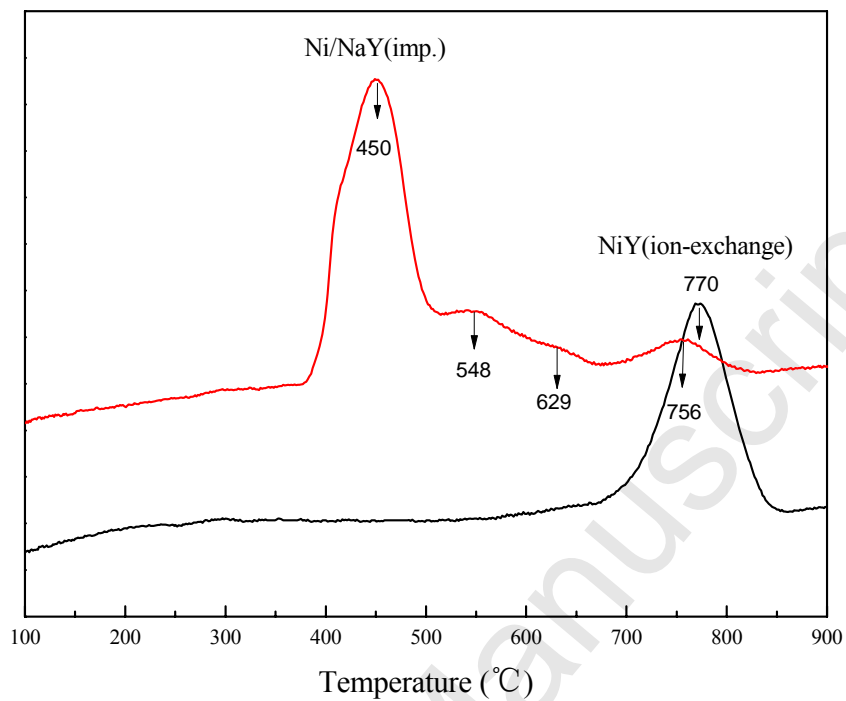


Fig. 2. TPR profiles of NiY and Ni/NaY catalysts. The peak at about 450 °C is due to the reduction of bulk NiO, the peak at 500–650 °C is attributed to the reduction of Ni ions located inside the channels of zeolite, the peak at 756 °C and 770 °C is due to the reduction of Ni sites incorporated into the zeolite framework

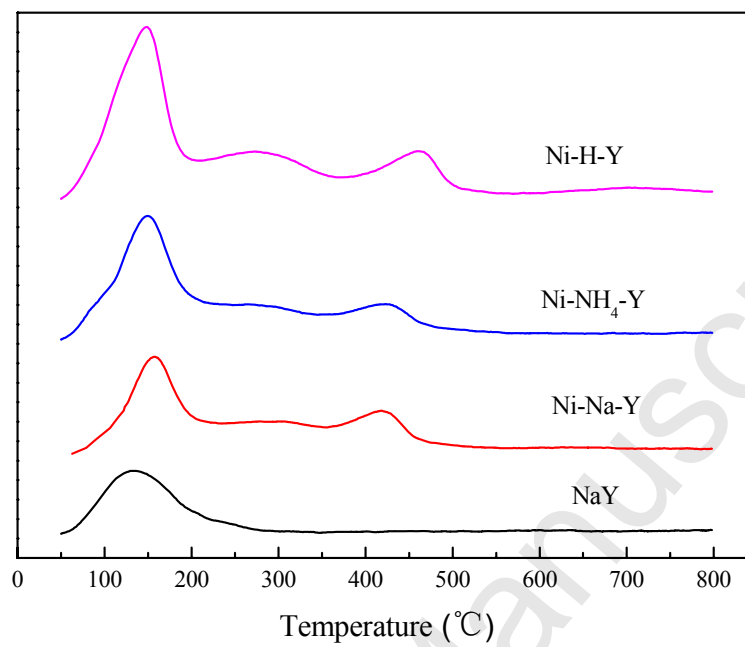


Fig. 3. NH₃-TPD profiles of NaY, NiY, Ni-NH₄Y and Ni-HY

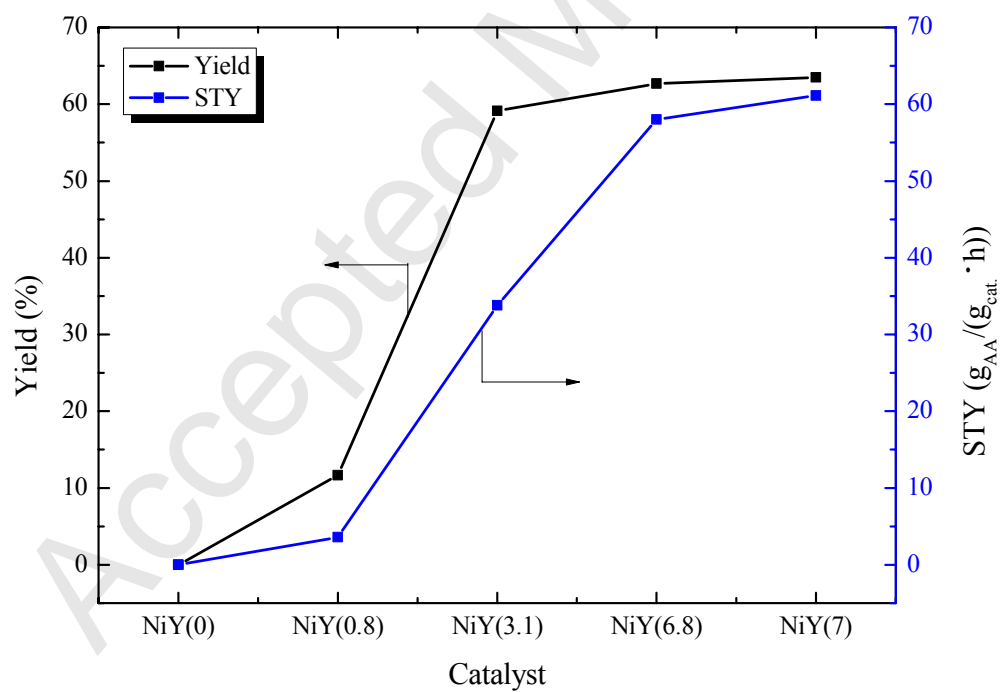


Fig. 4. Effect of Ni loading on catalytic activity (Reaction time: 120min for NiY(0), 90min for NiY(0.8), 64min for NiY(3.1), 44min for NiY(6.8), 40 min for NiY(7))

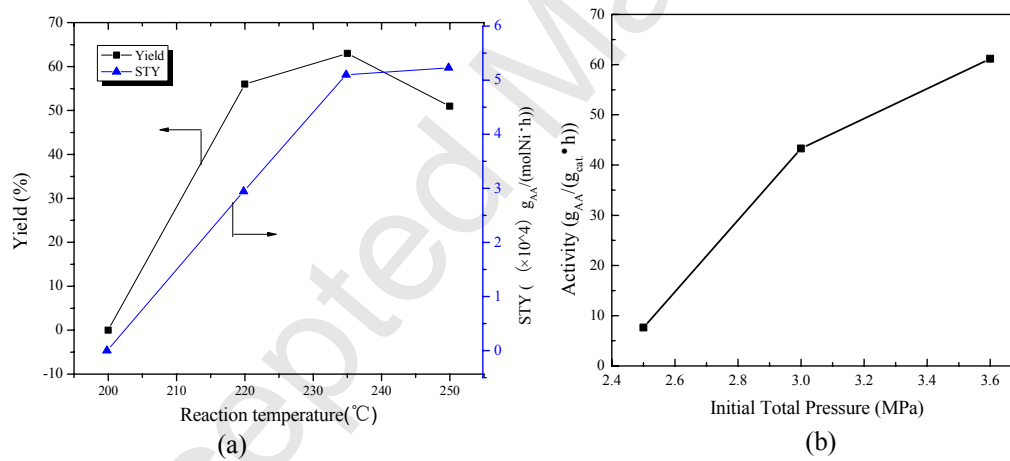


Fig. 5. Effect of reaction temperature (a) and initial total pressure (b) on the catalytic activity.

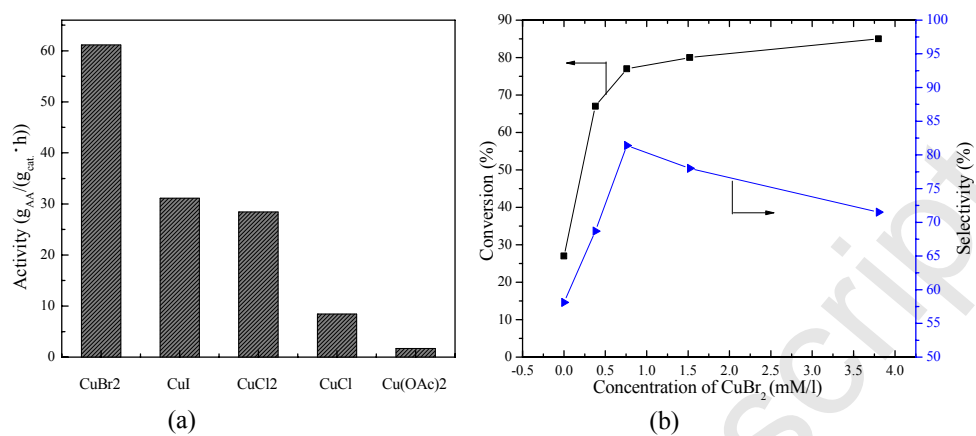


Fig. 6. Role of promoters in the hydrocarboxylation of acetylene: Effect of copper salts (a) and concentration of CuBr₂ (b) on the catalytic activity

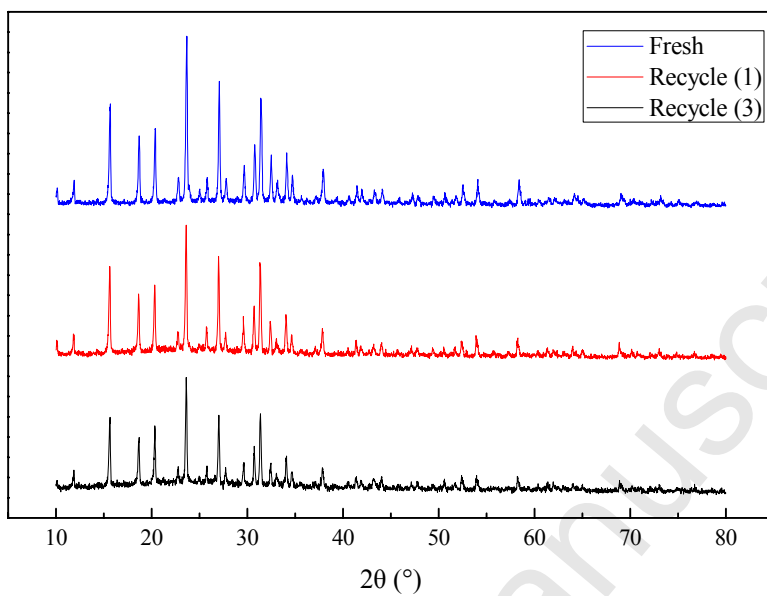


Fig. 7. X-ray diffraction patterns of the fresh and recovered NiY catalyst

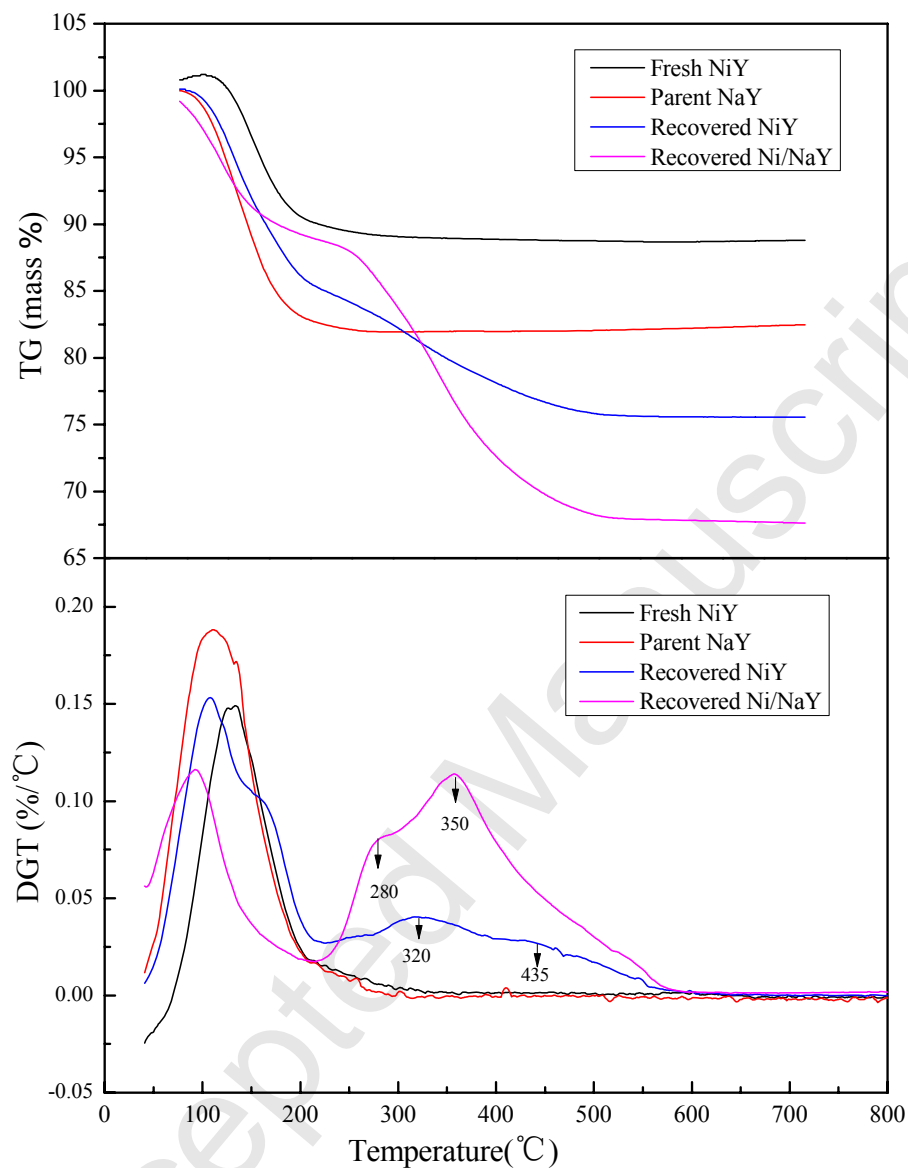


Fig. 8. Thermo gravimetric analysis of the fresh and spent Ni modified zeolite catalysts by ion-exchanged and wet impregnation: (A) weight loss as function of temperature (TG) and (B) derivative weight loss as function of temperature (DTG)

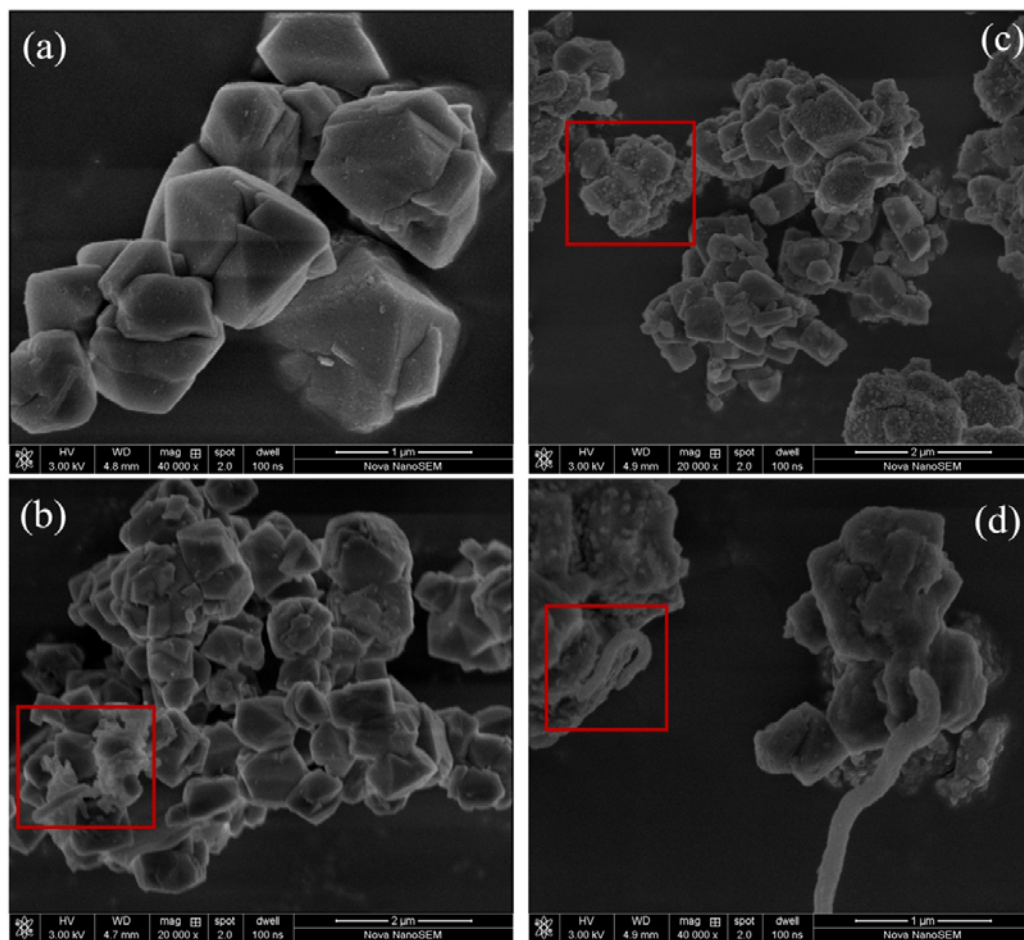


Fig. 9. SEM micrographs of fresh NiY(a) , recovered NiY(b) and recovered Ni/NaY(c,d)

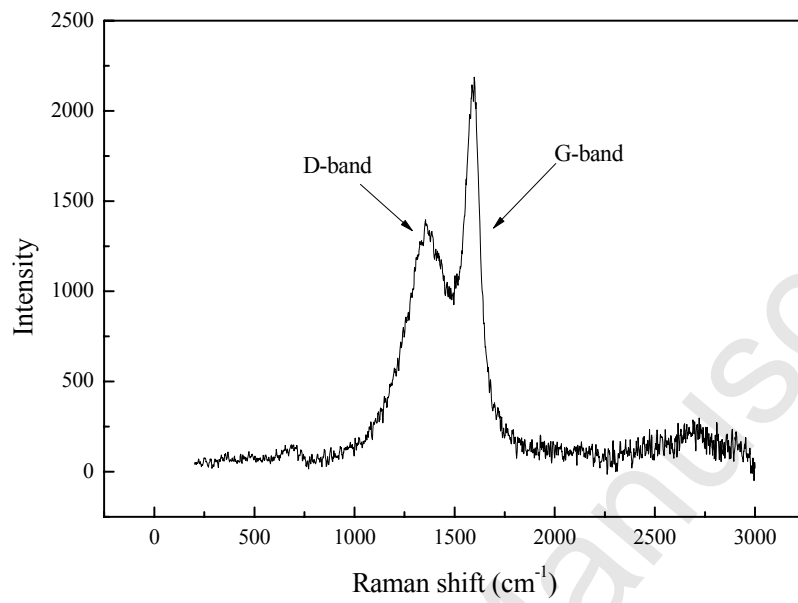
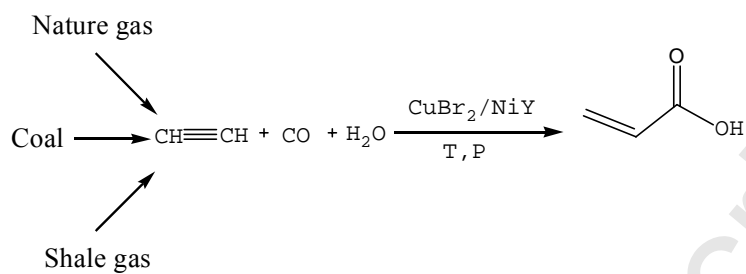


Fig. 10. Raman spectra of the recovered NiY catalyst

Graphical Abstract



Hydrocarboxylation of acetylene to acrylic acid over a cupric salt/NiY catalyst system